ORGANIC CHEMISTRY FRONTIERS

CCS 中国化学会 CHINESE CHEMICAL SOCIETY

SIOC 1950

ROYAL SOCIETY OF CHEMISTRY

RESEARCH ARTICLE

View Article Online
View Journal | View Issue

Cite this: *Org. Chem. Front.*, 2025, **12**, 1438

All-carbon supramolecular complexation of a bilayer molecular nanographene with [60] and [70]fullerenes†

Manuel Buendía, [a] Anton J. Stasyuk, [b,c] Salvatore Filippone, [a] Miquel Solà *[b] and Nazario Martín *[a,d]

Received 4th November 2024,
Accepted 24th December 2024

DOI: 10.1039/d4qo02071e

rsc.li/frontiers-organic

Supramolecular chemistry of carbon-based materials provides a variety of chemical structures with potential applications in materials science and biomedicine. Here, we explore the supramolecular complexation of fullerenes C_{60} and C_{70}, highlighting the ability of molecular nanographene tweezers to capture these structures. The binding constant for the **CNG-1⊃C$_{70}$** complex was significantly higher than for **CNG-1⊃C$_{60}$**, showing a clear selectivity for the more π-extended C_{70}. DFT calculations confirmed these experimental results by showing that the interaction energy of C_{70} with **CNG-1** is more than 5 kcal mol^{-1} higher than that of C_{60}. Theoretical calculations predict that the dispersion interaction provides about 58–59% of the total interaction energy, followed by electrostatic attraction with 26% and orbital interactions, which contribute 15–16%. The racemic nanographene tweezers effectively recognize fullerene molecules and hold promise for future applications in chiral molecule recognition.

Introduction

The supramolecular chemistry of carbon-based materials has been a recurring topic in organic chemistry with the uncountable possibilities and combinations stemming from the size and shape of graphene,[1,2] carbon nanotubes (CNTs),[3,4] and fullerenes.[5] As expected for these carbon nanostructures, non-covalent interactions such as C–H···π and, mostly, π···π interactions are those mainly controlling the formation of the resulting supramolecular ensembles.[6–9] Interestingly, the non-covalent functionalization of these carbon allotropes has provided a great variety of chemical architectures, many of them showing unexpected properties with potential biomedical[10] and materials science applications.[11]

In particular, the supramolecular complexation of fullerenes has received a lot of attention due to their singular spherical shape as well as their electron-acceptor nature, affording a variety of supramolecular complexes exhibiting new structural and optoelectronic properties.[6,12] Thus, a plethora of molecules of diverse structural complexity have been synthesized acting as hosts to capture guest fullerenes, especially C_{60} and C_{70}. In this regard, chemical structures based on macrocycles such as calixarenes,[13,14] cucurbiturils,[15] cyclodextrins,[16,17] molecular nanobelts,[18,19] cycloparaphenylenes (CPPs),[20–22] molecular cages,[23,24] as well as molecular tweezers endowed with curved π-extended moieties with positive Gaussian curvature such as corannulenes,[25] or with electronically complementary electron-donor molecules such as porphyrins or π-extended tetrathiafulvalenes (ex-TTFs)[26,27] have extensively been reported.

More recently, molecular nanographenes have attracted the attention of the scientific community due to their remarkable chiroptical and optoelectronic properties, their quick access and tunability through benchtop synthesis and their amazing structural diversity.[28–30] These nanometric fragments of graphene typically present a higher number of π–π interactions with fullerenes than other Polycyclic Aromatic Hydrocarbons (PAHs). Accordingly, molecular nanographenes have been used as hosts in host–guest chemistry with C_{60} and C_{70} species, being embedded into the aforementioned macrocycles as CPPs and nanobelts,[18,31,32] and also as simple molecules with either positive or negative Gaussian curvatures.[33] Interestingly, these supramolecular complexes not only have enhanced binding constants with fullerenes than their previous counterparts, but they can also showcase photoinduced electron transfer processes between the fullerene and the nanographene units.[34]

[a]*Departamento de Química Orgánica I, Facultad de Ciencias Químicas, Universidad Complutense de Madrid, Av. Complutense, S/N, 28040 Madrid, Spain. E-mail: nazmar@ucm.es*
[b]*Institut de Quimica Computacional i Catàlisi (IQCC) and Departament de Química, Universitat de Girona, M. Aurèlia Capmany, 69, 17003 Girona, Spain. E-mail: miquel.sola@udg.edu*
[c]*Departament de Farmàcia i Tecnologia Farmacèutica, i Fisicoquímica, Facultat de Farmàcia i Ciències de l'Alimentació & Institut de Química Teòrica i Computacional (IQTCUB), Universitat de Barcelona (UB), Av. Joan XXIII 27-31, Barcelona, Spain*
[d]*IMDEA-Nanociencia. C/Faraday, 9. Campus de Cantoblanco, 28049 Madrid, Spain*
† Electronic supplementary information (ESI) available. See DOI: https://doi.org/10.1039/d4qo02071e

In this work, we report on the molecular complexation of C_{60} and C_{70} with a molecular nanographene tweezer (**CNG-1**) as a suitable host previously obtained by a six-step synthetic process. Furthermore, theoretical calculations using the DFT BLYP exchange–correlation functional, along with the empirical D3(BJ) dispersion correction and def2-SVP basis set, nicely underpin the experimental values, matching the difference in interaction energy with binding constant values.

Results and discussion

Racemic and chiral triindane nanographene **CNG-1** was synthesized according to a procedure previously reported by our group.[35] Interestingly, this bilayer molecule exhibits a suitable concave geometry for further supramolecular complexation experiments. In particular, we envisaged to seize the inner cavity of this molecular tweezer with different fullerenes, namely C_{60} and C_{70}, endowed with complementary convex surfaces (Fig. 1).

The X-ray crystal structure of **CNG-1** revealed that both nanographene layers of the tweezer connected to the central triindane unit form an all-carbon host with an interlayer distance of around 9 Å, being a suitable host to accommodate either C_{60} or C_{70} fullerenes and, thus, affording their respective supramolecular complexes (Fig. 1). For this purpose, ^{1}H NMR titration experiments were performed to carry out the supramolecular complexation by following the evolution of the proton signals mostly affected in the complexation process between racemic **CNG-1** with fullerenes C_{60} and C_{70}.

These titration experiments were performed in deuterated chlorobenzene (PhCl-d^5) to ensure that both fullerene species were properly dissolved. Additionally, a complete NMR study was performed to assign all proton signals of **CNG-1** and gain a deeper insight into the complexation processes, which can be found in Fig. S1–S6, ESI.† The first titration involved **CNG-1** as host and fullerene C_{60} as guest. ^{1}H NMR spectra of this titration showcased chemical shifts of single time-averaged signals of **CNG-1** with additions up to 19 equivalents of guest C_{60}, evidencing a fast exchange rate in solution between complex and free host and guest species as well as the supramolecular complexation process (Fig. S7†). Notable differences in chemical shifts were observed for six proton signals: two *tert*-butyl protons ($\mathbf{H_a}$: δ_0 = 1.26 ppm; $\mathbf{H_b}$: δ_0 = 1.58 ppm), the less shielded methylene proton of the AB system ($\mathbf{H_c}$: δ_0 = 2.76 ppm), the doubly benzylic protons of the stereogenic centers ($\mathbf{H_d}$: δ_0 = 3.79 ppm), and two notably deshielded protons from the edge of the nanographene layers ($\mathbf{H_e}$: δ_0 = 8.82 ppm; $\mathbf{H_f}$: δ_0 = 9.30 ppm). The highest chemical shift difference was found for signal $\mathbf{H_c}$ ($\Delta\delta$ = 0.087 ppm) which, according to the X-ray data, belongs to the proton pointing towards the inner cavity of the nanographene tweezer, nicely confirming the complexation process (Fig. 2).

After plotting the titration data using *BindFit* fitting tool,[36,37] the non-linear fit afforded a moderate binding constant of K_a = 61 ± 1 M^{-1} for the **CNG-1⊃C$_{60}$** supramolecular complex, matching a 1 : 1 stoichiometry model (Nelder Mead method, Fig. S8;† for molar fraction evolution of both host and complex see Fig. S9†), thus confirming the affinity of **CNG-1** for fullerene C_{60}.

The second titration involving fullerene C_{70} as guest revealed a similar behavior for **CNG-1** host proton signals, where the same six signals from the first titration with C_{60} also shifted largely (Fig. S10†), with the greatest difference in chemical shift for the methylene signal $\mathbf{H_c}$ as well (δ_0 = 2.76 ppm, $\Delta\delta$ = 0.049 ppm). Moreover, complete saturation of complex in solution was reached (8 equivalents of C_{70}) as the $\mathbf{H_c}$ signal remained invariable, thus completing a successful titration (Fig. 3).

The non-linear adjust of these data resulted in a binding constant of K_a = 400 ± 17 M^{-1} for the **CNG-1⊃C$_{70}$** supramolecular complex, also matching with a 1 : 1 stoichiometry model (Nelder Mead method, Fig. S11;† for molar fraction evolution of both host and complex see Fig. S12†). This result demonstrates the higher affinity of **CNG-1** C_{70} over C_{60} with a binding constant value around one order of magnitude higher. Such enhancement can be accounted for by the larger π-extended surface of the C_{70} guest compared to the former C_{60} and,

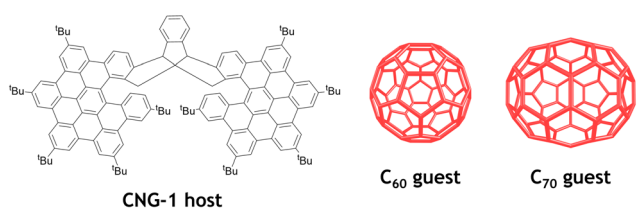

Fig. 1 All-carbon nanostructures involved in the supramolecular complexation of **CNG-1** with fullerenes C_{60} and C_{70}.

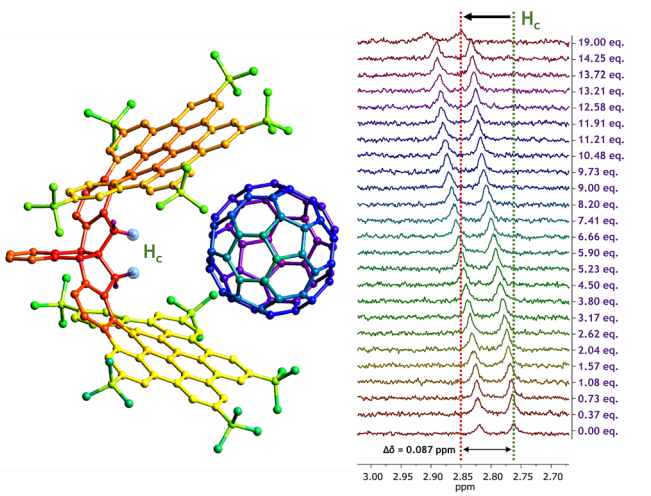

Fig. 2 Model for the supramolecular complexation of the **CNG-1⊃C$_{60}$** complex with a 1 : 1 stoichiometry (left), and $\mathbf{H_c}$ signal chemical shift variation upon addition of C_{60} equivalents throughout the titration in PhCl-d^5 (right).

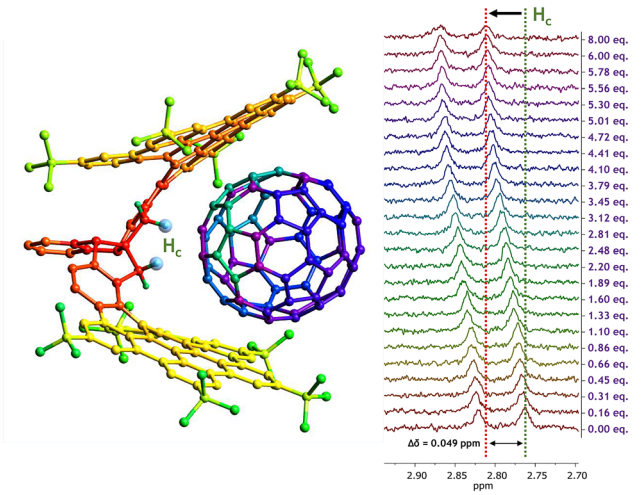

Fig. 3 Model for the supramolecular complexation of the **CNG-1⊃C$_{70}$** complex with a 1 : 1 stoichiometry (left), and **H$_c$** signal chemical shift variation upon addition of C$_{70}$ equivalents throughout the titration in PhCl-d^5 (right).

hence, increasing the π–π interactions between host **CNG-1** and guest C$_{70}$ molecules.

To gain insight into the nature of these supramolecular complexation processes, a series of quantum chemical calculations were performed. Systems of interest were optimized utilizing the DFT BLYP[38,39] exchange–correlation functional along with the empirical D3(BJ) dispersion correction[40,41] and def2-SVP basis set.[42,43] The calculations were performed within the ORCA 5.0.3 program[44] (see ESI for more details on the computational method used†).

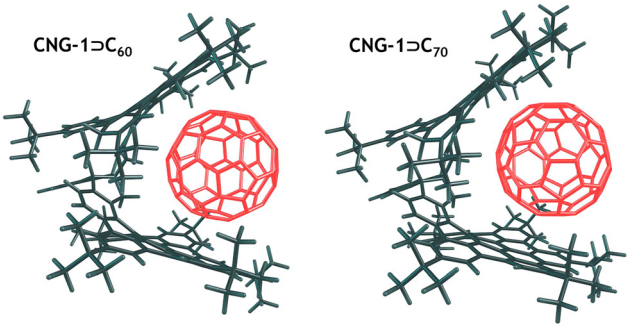

Fig. 4 Optimized DFT structures for supramolecular complexes **CNG-1⊃C$_{60}$** and **CNG-1⊃C$_{70}$**.

To assess the stability of the complexes, we calculated the interaction energy (ΔE_{int}) between the **CNG-1** tweezers and the C$_{60}$/C$_{70}$ units, as well as the deformation energy (ΔE_{def}) associated with the deformation of the units from their equilibrium geometries to the geometries they adopt in the complexes. DFT optimized structures of both complexes are provided in Fig. 4. For **CNG-1⊃C$_{60}$** and **CNG-1⊃C$_{70}$**, ΔE_{int} was found to be −61.3 and −66.1 kcal mol^{-1}, while ΔE_{def} was 3.1 and 2.5 kcal mol^{-1}, respectively (Table 1).

Most of the deformation energy is attributed to the **CNG-1** deformation, with deformation of the fullerenes contributing only 11 to 12%. It is interesting to note that despite the significant difference in the spatial sizes of C$_{60}$ and C$_{70}$ fullerenes, the deformation energy of the host unit in both complexes is nearly the same. This can apparently be explained by the mutual arrangement of the fullerenes and **CNG-1** units in the complexes. In particular, C$_{70}$ in the **CNG-1⊃C$_{70}$**, complex is positioned in such a way that its main axis runs along the cavity of the tweezers, and thus, the effective size of both fullerenes appears to be very similar.

To analyze the nature of the host–guest interactions, we employed the Morokuma-like interaction energy decomposition analysis (EDA)[45] implemented in the ADF program.[46] The EDA decomposes the interaction energy into four components: electrostatic (ΔE_{elstat}), Pauli repulsion (ΔE_{Pauli}), orbital interactions (ΔE_{oi}), and dispersion correction (ΔE_{disp}).[47] This decomposition enables us to assess the role of the specific interactions in the systems. Table 1 shows the EDA analysis results for **CNG-1⊃C$_{60}$** and **CNG-1⊃C$_{70}$** complexes.

As expected for both complexes, the nature of the host–guest interactions is nearly the same. In particular, dispersion interaction provides about 58–59% of the total interaction energy, followed by electrostatic attraction with 26%, and orbital interactions which contribute 15–16%. The destabilizing term (ΔE_{Pauli}) is slightly larger for **CNG-1⊃C$_{70}$** than for **CNG-1⊃C$_{60}$**, 116.9 and 104.6 kcal mol^{-1}, respectively. However, this difference is compensated to a significant extent by a larger dispersion correction term for **CNG-1⊃C$_{70}$** (Table 1). Overall, based on the complexation energy values, the **CNG-1⊃C$_{70}$** complex is more stable than **CNG-1⊃C$_{60}$** by 5.5 kcal mol^{-1}, supporting the higher binding constant for the complex with C$_{70}$ fullerene observed in the titration experiment.

Table 1 EDA results (in kcal mol^{-1}) and experimentally determined binding constant values (K_a) for **CNG-1⊃C$_{60}$** and **CNG-1⊃C$_{70}$** complexes[a]

	Energy terms					ΔE_{def}			
Complex	ΔE_{Pauli}	ΔE_{elstat}	ΔE_{oi}	ΔE_{disp}	ΔE_{int}	Host	C_{xx}	$\Delta E_{complex}$	K_a, M^{-1}
CNG-1⊃C$_{60}$	104.56	−43.24 (26%)	−25.80 (16%)	−96.78 (58%)	−61.25	2.74	0.37	−58.14	61 ± 1
CNG-1⊃C$_{70}$	116.86	−47.36 (26%)	−28.01 (15%)	−107.57 (59%)	−66.08	2.18	0.27	−63.63	400 ± 17

[a] Relative values (in parentheses) are given as a percentage and express the contribution to the sum of all attractive energy terms: $\Delta E_{elstat} + \Delta E_{oi} + \Delta E_{disp}$. Complexation energy: $\Delta E_{complex} = \Delta E_{int} + \Delta E_{def}$.

The analysis of the host–guest interaction topology for the complexes of interest, performed using the non-covalent interaction (NCI) index analysis,[48] revealed two distinct types of areas between the fullerenes and the **CNG-1** host unit. One type of these areas is located between the fullerene and the nanographene units of the tweezer.

Considering the π-conjugated nature of the fullerene and nanographene units, the interactions can be assigned as π···π interactions. The other type of area can be classified as C–H···π interactions due to its location between the fullerene and the hydrogen atoms of the central triindane fragment or the hydrogen atoms of the *tert*-butyl groups. The NCI isosurfaces for both complexes are presented in Fig. S13, ESI.†

Although these binding constants are lower with respect to other previously reported in literature for molecular nanographenes,[49] it is important to remark that **CNG-1** as a molecular receptor for fullerenes (especially C_{70}) is endowed with an inherent chiral triindane which, eventually, could open a door for the selective supramolecular recognition of sp^2 carbon-based chiral molecules.

Conclusions

The supramolecular complexation of guest fullerenes C_{60} and C_{70} with racemic molecular nanographene **CNG-1** as a host is presented in this work. Relatively moderate binding constant values were afforded for **CNG-1⊃C$_{60}$** and larger for **CNG-1⊃C$_{70}$** complexes, both accommodating the respective guest fullerene inside its cavity with a 1 : 1 stoichiometry. Moreover, the binding constant for **CNG-1⊃C$_{70}$** was one order of magnitude higher than that of **CNG-1⊃C$_{60}$**, thus revealing a clear selectivity towards the more π-extended fullerene. DFT calculations supported these experimental values, matching the difference in interaction energy with binding constant values. In this manner, we have demonstrated that racemic molecular nanographene **CNG-1**, can be used for the supramolecular recognition of carbon-based π-extended molecules such as fullerenes. Besides, its inherent chirality could potentially play a major role in the near future for the recognition of chiral molecules, including fullerenes.

Experimental section

Materials and methods

CNG-1 was prepared according to the procedure reported in the literature.[35] ^{1}H NMR spectra of the titration were recorded at 300 (Bruker AVIII) MHz at 298 K using deuterated chlorobenzene (PhCl-d^5) as solvent. All titrations were performed in an NMR sample tube charged with 0.5 mL of a starting **CNG-1** host solution (5×10^{-4} M). Sequential aliquots of a guest stock solution were added to the initial solution of **CNG-1** with a micropipette and mixing properly, recording their ^{1}H NMR spectra afterwards. These guest fullerene stock solutions were prepared dissolving the respective fullerene with a **CNG-1** solution of the same molarity as the initial to prevent dilution factors and keep a constant host concentration throughout the titration. Therefore, C_{60} + **CNG-1** (9.5×10^{-3} M and 5×10^{-4} M, respectively) and C_{70} + **CNG-1** (4×10^{-3} M and 5×10^{-4} M, respectively) stock solutions were afforded. The resulting titration data was fitted using *BindFit* fitting tool to determine the association constants.[37]

Data availability

The data supporting this article have been included as part of the ESI.†

Conflicts of interest

There are no conflicts to declare.

Acknowledgements

A. J. S. and M. S. thanks the Ministerio de Ciencia, Innovación y Universidades (MCIN/AEI/10.13039/50110001103) (Projects PID2023-147424NB-I00, PID2023-146849NB-I00, RED2022-134939-T, and FPI predoctoral grant to C. C.) and the Generalitat de Catalunya (Project 2021-SGR-623). A. J. S. gratefully acknowledge Polish high-performance computing infrastructure PLGrid (HPC Center: ACK Cyfronet AGH) for providing computer facilities and support within computational grant no. PLG/2023/016841.

M. B., S. F., and N. M. acknowledge financial support from the Spanish MICIN (project PID2020-114653RB-I00), they also acknowledge financial support from the ERC (SyG TOMATTO ERC-2020-951224) and from the '(MAD2D-CM)-UCM' project funded by Comunidad de Madrid, by the Recovery, Transformation and Resilience Plan and by NextGenerationEU from the European Union. M. B. also acknowledges financial support from the Spanish MICIN (project CTQ2017-83531-R).

References

1 K. S. Novoselov, A. K. Geim, S. V. Morozov, D. Jiang, Y. Zhang, S. V. Dubonos, I. V. Grigorieva and A. A. Firsov, Electric field effect in atomically thin carbon films, *Science*, 2004, **306**, 666–669.

2 A. K. Geim and K. S. Novoselov, The rise of graphene, *Nat. Mater.*, 2007, **6**, 183–191.

3 S. Iijima, Helical Microtubules of Graphitic Carbon, *Nature*, 1991, **354**, 56–58.

4 D. S. Bethune, C. H. Kiang, M. S. de Vries, G. Gorman, R. Savoy, J. Vazquez and R. Beyers, Cobalt-catalysed growth of carbon nanotubes with single-atomic-layer walls, *Nature*, 1993, **363**, 605–607.

5 H. W. Kroto, J. R. Heath, S. C. O'Brien, R. F. Curl and R. E. Smalley, C_{60}: Buckminsterfullerene, *Nature*, 1985, **318**, 162–163.
6 J. F. Nierengarten and N. Martín, *Supramolecular Chemistry of Fullerenes and Carbon Nanotubes*, Wiley, Weinheim, 2012.
7 E. M. Pérez and N. Martín, π-π interactions in carbon nanostructures, *Chem. Soc. Rev.*, 2015, **44**, 6425–6433.
8 V. Georgakilas, J. N. Tiwari, K. C. Kemp, J. A. Perman, A. B. Bourlinos, K. S. Kim and R. Zboril, Noncovalent Functionalization of Graphene and Graphene Oxide for Energy Materials, Biosensing, Catalytic, and Biomedical Applications, *Chem. Rev.*, 2016, **116**, 5464–5519.
9 G. Bottari, M. A. Herranz, L. Wibmer, M. Volland, L. Rodriguez-Perez, D. M. Guldi, A. Hirsch, N. Martin, F. D'Souza and T. Torres, Chemical functionalization and characterization of graphene-based materials, *Chem. Soc. Rev.*, 2017, **46**, 4464–4500.
10 Z. Liu, X. Sun, N. Nakayama-Ratchford and H. Dai, Supramolecular Chemistry on Water-Soluble Carbon Nanotubes for Drug Loading and Delivery, *ACS Nano*, 2007, **1**, 50–56.
11 L. von Luders, R. Tilmann, K. Lee, C. Bartlam, T. Stimpel-Lindner, T. K. Nevanen, K. Iljin, K. C. Knirsch, A. Hirsch and G. S. Duesberg, Functionalisation of Graphene Sensor Surfaces for the Specific Detection of Biomarkers, *Angew. Chem., Int. Ed.*, 2023, **62**, e202219024.
12 X. Chang, Y. Xu and M. von Delius, Recent advances in supramolecular fullerene chemistry, *Chem. Soc. Rev.*, 2024, **53**, 47–83.
13 J. L. Atwood, G. A. Koutsantonis and C. L. Raston, Purification of C_{60} and C_{70} by selective complexation with calixarenes, *Nature*, 1994, **368**, 229–231.
14 X.-S. Ke, T. Kim, V. M. Lynch, D. Kim and J. L. Sessler, Flattened Calixarene-like Cyclic BODIPY Array: A New Photosynthetic Antenna Model, *J. Am. Chem. Soc.*, 2017, **139**, 13950–13956.
15 F. Constabel and K. E. Geckeler, Solvent-free self-assembly of C_{60} and cucurbit[7]uril using high-speed vibration milling, *Tetrahedron Lett.*, 2004, **45**, 2071–2073.
16 T. Andersson, K. Nilsson, M. Sundahl, G. Westman and O. Wennerström, C_{60} embedded in γ-cyclodextrin: a water-soluble fullerene, *J. Chem. Soc., Chem. Commun.*, 1992, 604–606.
17 Z. Hu, C. Wang, F. Zhao, X. Xu, S. Wang, L. Yu, D. Zhang and Y. Huang, Fabrication of a graphene/C_{60} nanohybrid via gamma-cyclodextrin host-guest chemistry for photodynamic and photothermal therapy, *Nanoscale*, 2017, **9**, 8825–8833.
18 D. Lu, G. Zhuang, H. Wu, S. Wang, S. Yang and P. Du, A Large π-Extended Carbon Nanoring Based on Nanographene Units: Bottom-Up Synthesis, Photophysical Properties, and Selective Complexation with Fullerene C_{70}, *Angew. Chem., Int. Ed.*, 2017, **56**, 158–162.
19 X. Lu, T. Y. Gopalakrishna, Y. Han, Y. Ni, Y. Zou and J. Wu, Bowl-Shaped Carbon Nanobelts Showing Size-Dependent Properties and Selective Encapsulation of C_{70}, *J. Am. Chem. Soc.*, 2019, **141**, 5934–5941.
20 T. Iwamoto, Y. Watanabe, T. Sadahiro, T. Haino and S. Yamago, Size-selective encapsulation of C_{60} by [10]cycloparaphenylene: formation of the shortest fullerene-peapod, *Angew. Chem., Int. Ed.*, 2011, **50**, 8342–8344.
21 J. S. Wossner, D. Wassy, A. Weber, M. Bovenkerk, M. Hermann, M. Schmidt and B. Esser, [n] Cyclodibenzopentalenes as Antiaromatic Curved Nanocarbons with High Strain and Strong Fullerene Binding, *J. Am. Chem. Soc.*, 2021, **143**, 12244–12252.
22 M. Hermann, D. Wassy and B. Esser, Conjugated Nanohoops Incorporating Donor, Acceptor, Hetero- or Polycyclic Aromatics, *Angew. Chem., Int. Ed.*, 2021, **60**, 15743–15766.
23 Y. Shi, K. Cai, H. Xiao, Z. Liu, J. Zhou, D. Shen, Y. Qiu, Q. H. Guo, C. Stern, M. R. Wasielewski, F. Diederich, W. A. Goddard 3rd and J. F. Stoddart, Selective Extraction of C_{70} by a Tetragonal Prismatic Porphyrin Cage, *J. Am. Chem. Soc.*, 2018, **140**, 13835–13842.
24 C. García-Simón, M. Costas and X. Ribas, Metallosupramolecular receptors for fullerene binding and release, *Chem. Soc. Rev.*, 2016, **45**, 40–62.
25 A. Sacristán-Martín, D. Miguel, A. Díez-Varga, H. Barbero and C. M. Álvarez, From Induced-Fit Assemblies to Ternary Inclusion Complexes with Fullerenes in Corannulene-Based Molecular Tweezers, *J. Org. Chem.*, 2022, **87**, 16691–16706.
26 E. M. Pérez and N. Martín, Curves ahead: molecular receptors for fullerenes based on concave-convex complementarity, *Chem. Soc. Rev.*, 2008, **37**, 1512–1519.
27 E. Huerta, H. Isla, E. M. Pérez, C. Bo, N. Martín and J. de Mendoza, Tripodal exTTF-CTV hosts for fullerenes, *J. Am. Chem. Soc.*, 2010, **132**, 5351–5353.
28 L. Chen, Y. Hernandez, X. Feng and K. Müllen, From nanographene and graphene nanoribbons to graphene sheets: chemical synthesis, *Angew. Chem., Int. Ed.*, 2012, **51**, 7640–7654.
29 A. Narita, X. Y. Wang, X. Feng and K. Müllen, New advances in nanographene chemistry, *Chem. Soc. Rev.*, 2015, **44**, 6616–6643.
30 J. M. Fernández-García, P. Izquierdo-García, M. Buendía, S. Filippone and N. Martín, Synthetic chiral molecular nanographenes: the key figure of the racemization barrier, *Chem. Commun.*, 2022, **58**, 2634–2645.
31 Q. Huang, G. Zhuang, H. Jia, M. Qian, S. Cui, S. Yang and P. Du, Photoconductive Curved-Nanographene/Fullerene Supramolecular Heterojunctions, *Angew. Chem., Int. Ed.*, 2019, **58**, 6244–6249.
32 J. P. Mora-Fuentes, M. D. Codesal, M. Reale, C. M. Cruz, V. G. Jiménez, A. Sciortino, M. Cannas, F. Messina, V. Blanco and A. G. Campaña, Heptagon-Containing Nanographene Embedded into [10]Cycloparaphenylene, *Angew. Chem., Int. Ed.*, 2023, **62**, e202301356.
33 S. Zank, J. M. Fernández-García, A. J. Stasyuk, A. A. Voityuk, M. Krug, M. Solà, D. M. Guldi and N. Martín, Initiating

Electron Transfer in Doubly Curved Nanographene Upon Supramolecular Complexation of C_{60}, *Angew. Chem., Int. Ed.*, 2022, **61**, e202112834.

34 G. M. Beneventi, M. Krug, D. Reger, N. Jux and D. M. Guldi, Towards understanding the competition of electron and energy transfer in "molecular" nanographenes on the example of hexa-peri-hexabenzocoronene, *J. Photochem. Photobiol., C*, 2023, **56**, 100602.

35 M. Buendía, J. M. Fernández-García, J. Perles, S. Filippone and N. Martín, Enantioselective synthesis of a two-fold inherently chiral molecular nanographene, *Nat. Synth.*, 2024, **3**, 545–553.

36 A. J. Lowe, F. M. Pfeffer and P. Thordarson, Determining binding constants from ^{1}H NMR titration data using global and local methods: a case study using [n]polynorbornane-based anion hosts, *Supramol. Chem.*, 2012, **24**, 585–594.

37 D. B. Hibbert and P. Thordarson, The death of the Job plot, transparency, open science and online tools, uncertainty estimation methods and other developments in supramolecular chemistry data analysis, *Chem. Commun.*, 2016, **52**, 12792–12805.

38 A. D. Becke, Density-functional exchange-energy approximation with correct asymptotic behavior, *Phys. Rev. A*, 1988, **38**, 3098–3100.

39 C. Lee, W. Yang and R. G. Parr, Development of the Colle-Salvetti correlation-energy formula into a functional of the electron density, *Phys. Rev. B: Condens. Matter Mater. Phys.*, 1988, **37**, 785–789.

40 S. Grimme, J. Antony, S. Ehrlich and H. Krieg, A consistent and accurate ab initio parametrization of density functional dispersion correction (DFT-D) for the 94 elements H-Pu, *J. Chem. Phys.*, 2010, **132**, 154104.

41 S. Grimme, S. Ehrlich and L. Goerigk, Effect of the damping function in dispersion corrected density functional theory, *J. Comput. Chem.*, 2011, **32**, 1456–1465.

42 F. Weigend and R. Ahlrichs, Balanced basis sets of split valence, triple zeta valence and quadruple zeta valence quality for H to Rn: Design and assessment of accuracy, *Phys. Chem. Chem. Phys.*, 2005, **7**, 3297–3305.

43 F. Weigend, Accurate Coulomb-fitting basis sets for H to Rn, *Phys. Chem. Chem. Phys.*, 2006, **8**, 1057–1065.

44 F. Neese, Software update: The ORCA program system—Version 5.0, *Wiley Interdiscip. Rev.: Comput. Mol. Sci.*, 2022, **12**, e1606.

45 K. Morokuma, Why do molecules interact? The origin of electron donor-acceptor complexes, hydrogen bonding and proton affinity, *Acc. Chem. Res.*, 1977, **10**, 294–300.

46 ADF, *SCM, Theoretical Chemistry*, Vrije Universiteit, Amsterdam, The Netherlands, 2017, **https://www.scm.com**.

47 F. M. Bickelhaupt and K. N. Houk, Analyzing Reaction Rates with the Distortion/Interaction-Activation Strain Model, *Angew. Chem., Int. Ed.*, 2017, **56**, 10070–10086.

48 E. R. Johnson, S. Keinan, P. Mori-Sánchez, J. Contreras-García, A. J. Cohen and W. Yang, Revealing Noncovalent Interactions, *J. Am. Chem. Soc.*, 2010, **132**, 6498–6506.

49 H. He, Y. J. Lee, Z. Zong, N. Liu, V. M. Lynch, J. Kim, J. Oh, D. Kim, J. L. Sessler and X.-S. Ke, Nanographene-Fused Expanded Carbaporphyrin Tweezers, *J. Am. Chem. Soc.*, 2024, **146**, 543–551.